Angular correlation of annihilation radiation associated with vacancy defects in 6*H*-SiC

A. Kawasuso*

Advanced Science Research Center, Japan Atomic Energy Research Institute, 1233, Watanuki, Takasaki, Gunma, 370-1292, Japan

T. Chiba

National Institute for Materials Science, Namiki, 1-1, Tsukuba, 305-0044, Japan

T. Higuchi

Mizuho Information and Research Institute, 2-3, Kanda, Nishikicho, Chiyoda-ku, Tokyo, 101-8843, Japan
(Received 18 November 2004; published 26 May 2005)

Electron-positron momentum distributions associated with vacancy defects in 6*H*-SiC after irradiation with 2-MeV electrons and annealing at 1000 °C have been studied using angular correlation of annihilation radiation measurements. It was confirmed that the above vacancy defects have dangling bonds along the *c* axis and the rotational symmetry around it. The first-principles calculation suggested that the vacancy defects are attributable to either carbon-vacancy-carbon-antisite complexes or silicon-vacancy-nitrogen pairs, while isolated carbon vacancies, silicon vacancies, and nearest neighbor divacancies are ruled out.

Extensive studies have been carried out to date on radiation-induced defects in SiC. Silicon vacancies (V_{Si}) and carbon vacancies (V_C) are two of the most primitive defects. Early electron spin resonance (ESR) studies suggested that isolated silicon vacancies disappear through two major processes: recombination with interstitials (~ 200 °C) and migration to sinks (>600 °C).[1] From theoretical considerations,[2,3] in the latter process, transformation of isolated silicon vacancies to complexes composed of carbon vacancies and carbon antisites ($V_C C_{Si}$) occurs preferentially rather than migration to sinks. ESR signals observed after high-temperature annealing are attributed to $V_C C_{Si}$ complexes.[4–6]

In positron annihilation spectroscopy (PAS) studies on electron-irradiated 6*H*- and 4*H*-SiC, one type of vacancy defects giving rise to a positron lifetime of approximately 200 ps is found to have a higher thermal stability than that of isolated silicon vacancies.[7–17] They survive even after annealing at 1000 °C and ultimately disappear by annealing at 1300 - 1500 °C. Hence, they are distinguished from isolated silicon vacancies. They are observed in 4*H*- and 6*H*-SiC, but not in 3*C*-SiC.[18] The positron annihilation intensity increases with hexagonality. From the positron lifetime and Doppler broadening measurements, it is proposed that these vacancy defects are V_{Si}-related complexes[15,16] or divacancies.[13] Although silicon-vacancy-nitrogen pairs ($V_{Si}N$) were also considered since early modified Lely-grown crystals were heavily doped with nitrogen (5×10^{17} cm^{-3}),[9,10] later studies with lightly nitrogen-doped epilayers (5×10^{15} cm^{-3}) demonstrated no significant reduction of the above vacancy defects.[15,16] Theoretical studies imply that $V_C C_{Si}$ complexes may be the origin of the above vacancy defects.[2,3] Actually, the positron lifetime responsible for $V_C C_{Si}$ complexes calculated by the atomic superposition method[19] is reported to be comparable to that for silicon vacancies (~ 200 ps).[17] However, no direct evidences for the generation of $V_C C_{Si}$ com-

plexes have been obtained so far by PAS. Thus, the detailed structure has not yet been clarified.

In this work, we studied the vacancy defects in 6H-SiC induced by irradiation and annealing at 1000 °C using two-dimensional angular correlation of annihilation radiation (2D-ACAR) technique. One advantage of 2D-ACAR is the capability to provide anisotropic features of electron momentum distributions associated with vacancy defects.[20] This technique has been used for identification of vacancy defects in GaAs[21,22] and Si.[23] We will show that the above vacancy defects have an anisotropic electron momentum distribution along the *c* axis.

Specimens used in this study were cut from a *n*-type 6*H*-SiC(0001) wafer doped with nitrogen purchased from Nippon Corporation. The net carrier density was 1×10^{17} cm^{-3} at room temperature. These were irradiated with 2-MeV electrons to a fluence of 3×10^{17} e$^-$/cm^2 at room temperature. Subsequently, a heat treatment was carried out at 1000 °C for 30 min in dry argon ambient. From the preliminarily positron lifetime measurements, we obtained a single positron lifetime of 140 ps. This is in good agreement with the bulk lifetime. After irradiation, two lifetime components were obtained: $\tau_1 = 110$ ps and $\tau_2 = 210$ ps with $I_2 = 75\%$ for the as-irradiated state and $\tau_1 = 116$ ps and $\tau_2 = 190$ ps with $I_2 = 69\%$ after annealing at 1000 °C. These are qualitatively in agreement with previous studies.[9,10] However, the bulk lifetime of 158 ps calculated within the two-state trapping model deviates from 140 ps. This discrepancy comes from uncertainties in the decomposition process of the lifetime spectrum due to the limited time resolution. Consequently, the positron trapping rate of 8.4 ns^{-1} was determined using the average lifetime.[20] Thus, the fraction of positrons trapped at vacancy defects (f) after annealing is 0.54. Positrons emitted from a ^{22}Na source with an activity of 840 MBq were injected to the specimens from the (0001) surface. The 2D-ACAR spectrum was obtained on the *x-z* plane at
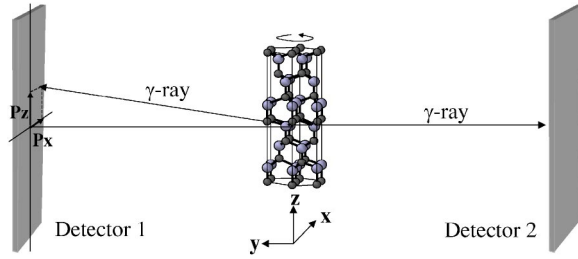
FIG. 1. Schematic representation of 6*H*-SiC and definition of orientation in 2D-ACAR measurement.

two crystal orientations $(x:[1\bar{1}00]-z:[0001];x:[11\bar{2}0]-z:[0001])$, as shown in Fig. 1. Annihilation gamma rays (511 keV) were detected by two position-sensitive Anger cameras separated 7 m away from the sample. Detecting coincidence events, ACAR spectra were measured at room temperature. The angular resolutions to x and z directions were 0.5 mrad and 1 mrad, respectively. Detailed topological features of ACAR spectra were visualized by the anisotropy plots as follows:

$$A(p_x,p_z) = N(p_x,p_z) - \frac{1}{2\pi}\int_0^{2\pi} N(p,\theta)d\theta, \quad (1)$$

where $N(p_x,p_z)$ is the 2D-ACAR spectrum, $p^2=p_x^2+p_z^2$ and $\theta=\arctan(p_z/p_x)$.

Figures 2(a) and 2(b) show the ACAR anisotropy spectra from the unirradiated sample at the $[1\bar{1}00]-[0001]$ and $[11\bar{2}0]-[0001]$ projections. Pronounced anisotropies related

to the momentum distribution of valence electrons are seen. After electron irradiation, these crystal-related anisotropies diminished and different anisotropies appear. This is due to the increase in the annihilation probability of positrons at vacancy defects. To extract anisotropies related to vacancy defects, the crystal components were subtracted from the original spectra. The fraction of the vacancy component f', which is apparently distinguished from the crystal components, was determined by minimizing the following quantity:

$$\chi^2(f') - \int\int [A(p_x,p_z) - (1-f')A_C(p_x,p_z)]^2 dp_x dp_z, \quad (2)$$

where $A_C(p_x,p_z)$ is the ACAR anisotropy spectrum for the unirradiated sample ("*C*" denotes "crystal").[24] This method yields the vacancy fraction as long as its ACAR anisotropy adequately differs from that for the bulk.[25] Figures 2(c) and 2(d) show the ACAR anisotropy spectra coming from vacancy defects obtained after irradiation and annealing at 1000 °C. Here, the vacancy components are $f'=0.40$ for (c) and $f'=0.37$ for (d); i.e., practically the same. These vacancy fractions are underestimated as compared to that obtained from the positron lifetime ($f=0.54$). As discussed later, this is interpreted as the existence of the bulklike components for vacancy defects depending on the orientation.

The ACAR anisotropy spectra from vacancy defects shown in Figs. 2(c) and 2(d) are much different than those from the crystal. That is, the electron momentum distribution is anisotropic towards the c axis. This indicates that vacancy defects have dangling bonds orientated along the c axis. The ACAR anisotropy spectra at the $[1\bar{1}00]-[0001]$ and
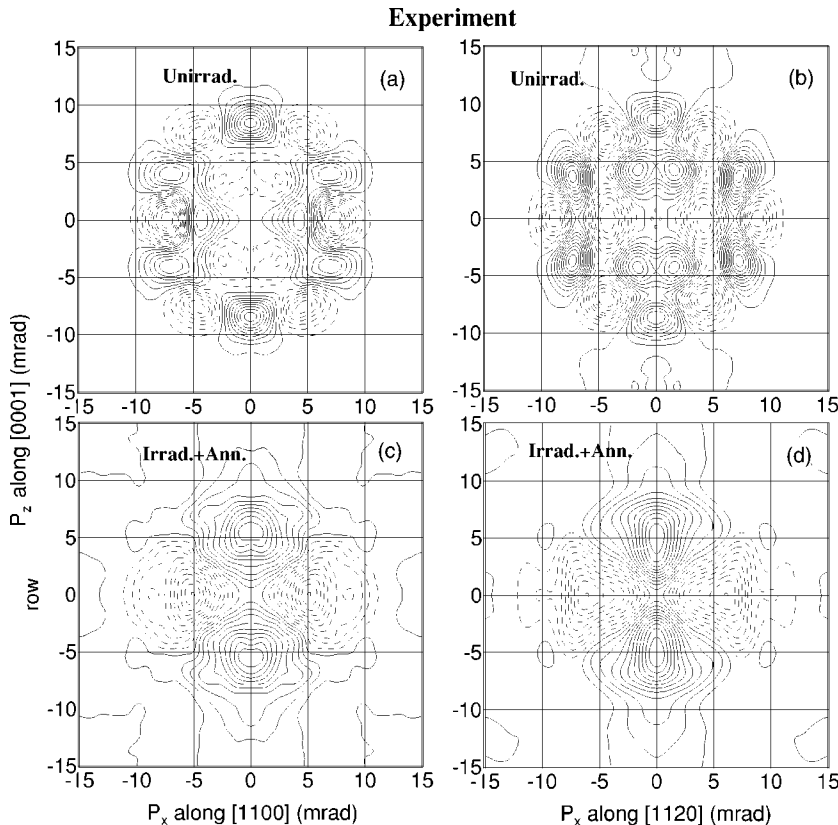
Experiment

FIG. 2. Experimental 2D-ACAR anisotropy spectra for unirradiated 6*H*-SiC at (a) the $[1\bar{1}00]-[0001]$ projection and (b) the $[11\bar{2}0]-[0001]$ projection. (c) and (d) show the spectra for the specimen irradiated with 2-MeV electrons to a fluence of 3×10^{17} e$^-$/cm^2 and annealed at 1000 °C for 30 min after subtracting the bulk components using Eq. (2). Solid and dashed lines represent positive and negative values, respectively. The contour spacing is 5% of the difference between maximum and minimum intensities.
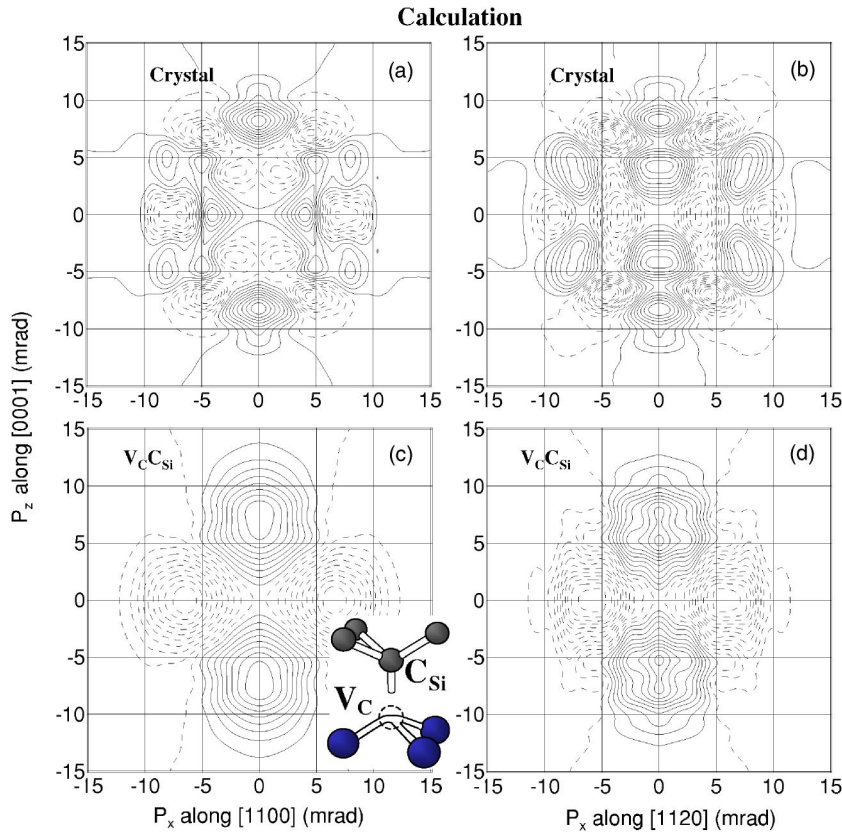
FIG. 3. Theoretical 2D-ACAR anisotropy spectra for a perfect lattice at (a) the $[1\bar{1}00]$–$[0001]$ projection and (b) the $[11\bar{2}0]$–$[0001]$ projection. Same for $V_C C_{Si}$ complexes, at (c) the $[1\bar{1}00]$–$[0001]$ projection and (d) the $[11\bar{2}0]$–$[0001]$ projection. Solid and dashed lines represent positive and negative values, respectively. The contour spacing is 5% of the difference between maximum and minimum intensities. The structure of $V_C C_{Si}$ complex is also shown schematically.

$[11\bar{2}0]$–$[0001]$ projections are different from each other. This relationship was conserved after rotating the crystal by 120° around the c axis. Thus, the electron momentum distribution holds the threefold rotational C_{3V} symmetry around the c axis.

The above observations were examined theoretically; the positron-electron momentum distribution was first calculated using the conventional scheme:[19]

$$\rho(\mathbf{p}) = \pi r_e c^2 \sum_{occ} \left| \int e^{-i\mathbf{pr}} \Psi_+(\mathbf{r}) \Psi_-(\mathbf{r}) \sqrt{\gamma(\mathbf{r})} d\mathbf{r} \right|^2, \quad (3)$$

where r_e is the classical electron radius, c is the light speed, $\Psi_+(\mathbf{r})$ is the positron wave function, $\Psi_-(\mathbf{r})$ is the electron wave function, and $\gamma(\mathbf{r})$ is the enhancement factor. We adopted the Broński-Nieminen enhancement factor.[26] The summation goes over all the occupied states. A supercell including 48 Si and 48 C atoms was constructed for the perfect lattice. The lattice constants were fixed at $a=3.08$ Å, $b=5.33$ Å, and $c=15.11$ Å.[27] The electron wave function was computed based on the norm-conserving pseudopotential method using the ABINIT4.1.4 code.[28] Only one k-point (Γ point) was considered. The cutoff energy of the plane-wave basis set was typically 40 Ryd. In the calculation of vacancies, to reach a rapid convergence, we did not move ion positions in the calculation. Instead, optimized geometrical data for the first nearest neighbor atoms provided by Bochstedte of Erlangen University were used as input.[29] A self-consistent positron wave function was calculated based on the two-component density functional theory so as to mini-

mize the energy functional.[26] 2D-ACAR spectra were subsequently obtained by integrating the momentum density in one particular momentum axis. Figures 3(a) and 3(b) show the calculated ACAR anisotropy spectra for the perfect crystal. The calculation reproduces well the observation in Figs. 2(a) and 2(b). The bulk positron lifetime (136 ps) was also confirmed to be in good agreement with experiment.

During the preliminary calculations, the observations shown in Figs. 2(c) and 2(d) were hardly reproduced considering carbon vacancies, silicon vacancies and nearest neighbor divacancies because of the absence of dangling bonds along the c axis after the reconstructions. On the contrary, the ACAR anisotropy spectra calculated for $V_C C_{Si}$ complexes exhibited the strong anisotropies along the V_C-C_{Si} line. No significant difference due to inequivalent lattice site was found. The axis of a $V_C C_{Si}$ complex has four orientations from the center of carbon vacant sites in the tetrahedron. That is, a C_{Si} can replace with one of the four silicon atoms around a V_C. The most pronounced ACAR anisotropies appeared when the V_C-C_{Si} line was parallel to the c axis. In the other cases, the ACAR anisotropy spectra were somewhat bulklike. Only in one case, where the $V_C C_{Si}$ line was on the (1120) plane, the axial orientation appeared in the $[1\bar{1}00]$–$[0001]$ projection. Consequently, the ACAR anisotropy spectra arising from $V_C C_{Si}$ complexes contain both prominent anisotropies along the c axis and bulklike anisotropies. Thus, we may consider the former case since the bulklike components may be mostly subtracted with the real bulk components, as described in Eq. (2).

Figures 3(c) and 3(d) show the ACAR anisotropy spectra calculated for $V_C C_{Si}$ complexes with the c-axis orientation.

Apparent anisotropies along the c axis are seen. These anisotropies along the c axis are mainly coming from the dangling bonds of carbon antisites. The different anisotropies in these figures are caused by the contribution from the rest reconstructed Si bonds. The calculated ACAR anisotropy spectra agree with the experiments. This implies the formation of $V_C C_{Si}$ complexes. Above, it was pointed that the vacancy fractions were underestimated as compared to the positron lifetime measurements. This is explained as the existence of bulklike anisotropies in the case that the V_C-C_{Si} line is not parallel to the c axis, as discussed above.

In the previous studies, $V_{Si} N_C$ pairs were also proposed as the origin for vacancy defects produced by post-irradiation annealing at 1000 °C in nitrogen-doped $6H$-SiC.[9,10] We therefore calculated ACAR anisotropy spectra for $V_{Si} N_C$ pairs with the atomic arrangements determined by Gerstmann *et al.*[30] For reasons similar to the case of $V_C C_{Si}$ complexes, anisotropies along the c axis appeared when the V_{Si}-N_C line was parallel to it. The overall ACAR distributions were very similar to those for $V_C C_{Si}$ complexes. Thus, the possibility of $V_{Si} N_C$ pairs is not completely denied from the ACAR anisotropy spectra although the vacancy defects are observed irrespective to nitrogen doping.

Linger *et al.* attributed the ESR signals from neutron-irradiated n-type $6H$-SiC to $V_C C_{Si}$ complexes.[4] This is consistent with the theoretical prediction that isolated silicon vacancies transform to $V_C C_{Si}$ complexes.[2,3] Their recent study shows that these complexes are annealed out below 1200 °C.[6] Zolnai *et al.* also showed that similar ESR signals in p-type $4H$-SiC disappear at 1100 °C.[5] These annealing temperatures are lower than the ultimate annealing temperature (1300–1500 °C) of the above PAS-detected vacancy defects. Thus, to conclude that the PAS-detected vacancy defects originate from $V_C C_{Si}$ complexes, we still need to examine the annealing behavior of both PAS and ESR-detected centers using practically identical samples.

In summary, we studied vacancy defects in $6H$-SiC induced by post-irradiation annealing at 1000 °C using 2D-ACAR technique. Pronounced anisotropies along the c axis related to vacancy defects were found. This suggests that these vacancy defects have dangling bonds oriented towards the c axis and the rotational symmetry around it. Both $V_C C_{Si}$ complexes and $V_{Si} N_C$ pairs were found to yield the comparable ACAR anisotropy spectra to the experiments. To discriminate these two candidates, the further studies are needed.

*Electronic address: ak@taka.jaeri.go.jp

[1] H. Itoh *et al.*, J. Appl. Phys. **66**, 4529 (1989).

[2] M. Bochstedte, A. Mattausch, and O. Pankratov, Phys. Rev. B **69**, 235202 (2004).

[3] E. Rauls *et al.*, Phys. Status Solidi B **217**, R1 (2000).

[4] T. Linger, S. G. Weber, and J. M. Spaeth, Phys. Rev. B **64**, 245212 (2001).

[5] Z. Zolnai *et al.*, Mater. Sci. Forum **457–460**, 473 (2004).

[6] M. V. B. Pinheiro *et al.*, Mater. Sci. Forum **457–460**, 517 (2004).

[7] A. I. Girka *et al.*, Sov. Phys. Semicond. **23**, 1337 (1989).

[8] A. A. Rempel and H. E. Schaefer, Appl. Phys. A: Mater. Sci. Process. **61**, 51 (1995).

[9] A. Kawasuso *et al.*, J. Appl. Phys. **80**, 5639 (1996).

[10] A. Kawasuso *et al.*, J. Appl. Phys. **82**, 3232 (1997).

[11] A. Kawasuso *et al.*, Mater. Sci. Forum **264–268**, 611 (1998).

[12] A. Kawasuso *et al.*, Appl. Phys. A: Mater. Sci. Process. **67**, 209 (1998).

[13] A. Polity, S. Huth, and M. Lausmann, Phys. Rev. B **59**, 10603 (1999).

[14] C. C. Ling, C. D. Beling, and S. Fung, Phys. Rev. B **62**, 8016 (2000).

[15] A. Kawasuso *et al.*, J. Appl. Phys. **90**, 3377 (2001).

[16] A. Kawasuso *et al.*, Appl. Phys. Lett. **79**, 3950 (2001).

[17] A. Kawasuso, in *Silicon Carbide -Recent Major Advances*, edited by W. J. Choyke, H. Matsunami, and G. Pensl (Springer-Verlag, Berlin, 2004), p. 563.

[18] A. Kawasuso *et al.*, Mater. Sci. Forum **433–436**, 477 (2002).

[19] M. J. Puska and R. M. Nieminen, Rev. Mod. Phys. **66**, 841 (1994).

[20] *Positron Annihilation in Semiconductors, Defect Studies*, edited by R. Krause-Rehberg and H. S. Leipner (Springer, Berlin, 1999), Vol. 127.

[21] L. Gilgien *et al.*, Phys. Rev. Lett. **72**, 3214 (1994).

[22] R. Ambigapathy *et al.*, Appl. Phys. A: Mater. Sci. Process. **62**, 529 (1996).

[23] Z. Tang *et al.*, Phys. Rev. Lett. **78**, 2236 (1997).

[24] T. Chiba *et al.*, in *Proceedings of the 3rd International Workshop on Positron Studies of Semiconductor Defects*, edited by Z. T. M. Hasegawa and Y. Nagai, 2003, p. 172.

[25] M. Hasegawa *et al.*, Mater. Sci. Forum **196–201**, 1481 (1995).

[26] E. Boroński and R. M. Nieminen, Phys. Rev. B **34**, 3820 (1986).

[27] A. Taylor and R. M. Jones, in *Silicon Carbide -A High Temperature Semiconductor*, edited by J. R. O'Connor and J. Smiltens (Pergamon, New York, 1960), p. 147.

[28] X. Gonze *et al.*, Comput. Mater. Sci. **25**, 478 (2002).

[29] M. Bochstedte (private communication).

[30] U. Gerstmann *et al.*, Phys. Rev. B **67**, 205202 (2003).